frontiers | Frontiers in Coatings, Dyes and Interface Engineering

TYPE Mini Review
PUBLISHED 02 May 2024
DOI 10.3389/frcdi.2024.1401391

OPEN ACCESS

EDITED BY
Robert Wood,
University of Southampton, United Kingdom

REVIEWED BY
Zhenxue Zhang,
University of Birmingham, United Kingdom

*CORRESPONDENCE
Angela De Bonis,
angela.debonis@unibas.it

RECEIVED 15 March 2024
ACCEPTED 17 April 2024
PUBLISHED 02 May 2024

CITATION
Curcio M, Teghil R and De Bonis A (2024), Thin-film microbattery fabrication by PLD: a comprehensive mini-review.
Front. Coat. Dye In. 2:1401391.
doi: 10.3389/frcdi.2024.1401391

Thin-film microbattery fabrication by PLD: a comprehensive mini-review

Mariangela Curcio, Roberto Teghil and Angela De Bonis*

Dipartimento di Scienze, Università della Basilicata, Potenza, Italy

This mini-review reports the latest results on Pulsed Laser Deposition (PLD) for the design and development of microbatteries. Advances in the deposition of thin films for cathodes, anodes and electrolytes are considered separately, the focus being on studies reporting the electrochemical characterization and performance of electroactive films. Some results on the positive effects of coatings to study and mitigate anode degradation are also discussed.

KEYWORDS

pulsed laser deposition, microbattery, cathodes, anodes, electrolytes

1 Introduction

A microbattery is a solid state battery (SSB) designed to provide power for small-scale electronic devices. SSB have significant advantages over conventional batteries in terms of performance, sustainability and safety due to their greater thermal and chemical stability, higher energy density, and absence of flammable liquids. Due to the increasing demand of flexible electronic microdevices such as implantable medical devices or skin patches, many researchers have been focused on the deposition of positive and negative electrodes and solid electrolytes for the development of microbatteries. Among micro-SSB, thin-film batteries (TFBs) typically feature a layer-by-layer stacked structure, where various components (cathode, electrolyte, and anode) are sequentially deposited onto a substrate, which can also serve as a current connector. To ensure efficient transfer of both electrical and ionic charge, the electrodes must be extremely thin (with a maximum thickness of a few microns), with the electrolyte even thinner. To achieve this, various deposition techniques have been explored, such as magnetron sputtering, pulsed laser deposition (PLD), thermal evaporation, chemical vapor deposition (CVD), atomic layer deposition (ALD), and printing (Xia et al., 2023). Within these, PLD is widely recognized as a versatile technique for the growth of films. Thanks to the possibility to deposit dense and pure films, PLD has gathered the attention of the scientist for the development of solid state batteries (SSB) (Julien and Mauger, 2019; Fenech and Sharma, 2020). In PLD, a pulsed laser beam ablates material from a solid target, depositing it onto a substrate in form of thin film. The interaction between the laser and target material causes laser photon absorption, leading to the vaporization of the superficial layers of the target and plasma formation, consisting in a mixture of atoms, molecules, ions, electrons, and clusters. The plasma's composition and expansion are closely linked to deposition parameters, particularly the ambient background (such as vacuum or background gas inert or reactive) and laser parameters (including pulse duration, wavelength, and fluence). Therefore composition, morphology, crystallinity and thickness of the obtained film can be tuned by controlling many experimental parameters during the deposition such as laser wavelength, energy and pulse length, deposition temperature and atmosphere and so on. The role of several PLD

parameters on the film's growth and properties has been discussed (Indrizzi et al., 2020). The advantages and drawbacks of PLD with respect to other chemical and physical deposition methodologies used for the growth of thin electroactive films, were recently reviewed (Karimzadeh et al., 2023; Xia et al., 2023). In brief, among the main advantages of PLD are: i) the ability to deposit any type of material for TFBs, ii) congruent transfer of composition, and iii) low deposition temperatures. However, scaling up production proves challenging as the film maintains its homogeneity over a limited area of the substrate.

This mini-review explores the studies published after 2019 focused on laser technologies for the development of batteries with different chemistry and microbatteries with enriched performances. The cathode, anodes and electrolytes components are separately considered. In particular we have considered studies that report the electrochemical characterization for anodes and cathodes. As the study of solid-state electrolytes is relatively recent compared to other components, only limited investigations on thin film electrolytes deposited via PLD are available, with some focusing solely on optimizing deposition parameters. Therefore, all papers have been considered, despite the absence of electrochemical studies. The experimental details for the deposition of cathodes, anodes and electrolytes are reported in Table 1. A schematic illustration of the sequential deposition process and the cross-section of a thin film battery is reported in Figure 1.

2 Cathodes

2.1 Cathodes for Lithium Ion Batteries

2.1.1 Transition metal oxides

Transition metal oxide (TMO) stands out as the most promising commercial cathode material for Lithium Ion Batteries (LIBs), moreover, thanks to their adjustable electrochemistry, reversible capacity, and easy synthesis process TMO resulted attractive also for Sodium Ion Batteries (SIBs). In particular, to the simplicity in varying the transition metal within the crystalline structure, which acts as the redox center, allows the electrochemical properties modulation through the utilization of different transition metals reference (Zhao et al., 2023).

Among various TMOs for LIBs, compounds like MoO_3, V_2O_5, and MnO_2 possess a structure that facilitates ionic intercalation, leading to satisfactory specific capacities. However, a primary issue lies in their low diffusion coefficient. Nanostructured forms offer a potential solution, reducing diffusion paths and increasing the number of reaction sites.

Mo_3 was deposited in an oxygen atmosphere at various pressures (2, 5, 10, and 20 Pa) to control the quantity of oxygen vacancies introduced into the cathodic film. The authors observed that as the oxygen pressure decreased, the percentage of oxygen vacancies increased, until the oxygen supply was sufficiently low to induce the formation of a less oxidized MO_2 phase. Whereas, the film deposited at 10 Pa exhibited the best electrochemical properties, demonstrating that a limited number of OVs leads to an improvement in electrochemical performance, due to the increased carrier density and reaction sites (Wei et al., 2023). Moreover by selecting appropriate substrates and deposition parameters it is possible to tune the crystal orientation of epitaxial MoO_3 thin films. It has been demonstrated that when the (011) and (102) planes are exposed to the electrolyte, ion intercalation is favored, leading to improved electrochemical properties compared to cathode film with (00 k) face exposed (Trzciński et al., 2023).

Hongliang et al. (2021) deposited V_2O_5 and V_2O_5-Au composite cathode. The latter is composed of 10 nm sized Au nanoparticles homogeneously anchored on V_2O_5 nanosheets. The cyclic voltammetry analysis of pure V_2O_5 and V_2O_5-Au electrodes reveals characteristic oxidation and reduction current peaks, consistent with the presence of α-V_2O_5. The comparison of cycling performance shows that the V_2O_5-Au electrode exhibits higher discharge capacity and better capacity retention attributed to enhanced electronic conductivity provided by gold nanoparticles: 78.7% and 83.5% for V_2O_5 and V_2O_5-Au, respectively (Hongliang et al., 2021).

Undoped and Sn-doped V_2O_5 thin films were deposited and subjected to a rapid thermal annealing in a reducing nitrogen atmosphere, which lead to the formation of a predominantly V_2O_3 phase. Sn-doped V_2O_3 film exhibited only a slight enhancement in initial capacity to 311 mAh/g. Whereas prolonged stability analysis revealed significant capacity decay in undoped V_2O_3 electrodes, while the incorporation of Sn^{4+} resulted in notable improvement in long-term stability, exhibiting more than twice the capacity retention compared to undoped electrodes (Tite et al., 2023).

$LiMn_2O_4$ (LMO) was deposited following a multi-layer PLD approach: with the aim to reduce the Li losses, commonly encountered during laser deposition due to its low mass, sequential layers of LMO e Li_2O (4:3) were deposited (Erinmwingbovo et al., 2020; Siller et al., 2022). Nonetheless, small amounts of MnO3 and non stoichiometric phases were detected in XRD analysis. However, Siller et al. (2022) have shown that these material defects resulting from deviation from stoichiometry have contributed to good cycling stability by ensuring a lower volume variation during charge and discharge processes.

Kuwata et al. (2022) investigated the electrochemical characteristics of LMO in a thin-film cell where each component was deposited via PLD: $Li/Li_3PO_4/LiMn_2O_4$. Through *in situ* Raman spectroscopy, they investigated the structural changes of LMO during charge and discharge cycles and their correlation with Li diffusion.

PLD of electrode materials is often performed to produce models for analyzing reaction mechanisms. In this regard, epitaxial thin films of Li_2MnO_3 with various Li/Mo ratios were deposited at different oxygen pressures, and the electrochemical processes were studied (Hikima et al., 2021). From structural and electrochemical analysis it was evidenced that reaction mechanisms in non stoichiometric Li_2MnO_3 differ from the stoichiometric one, which shown also lower degradation.

$LiCoO_2$ (LCO) is a primary cathode active material characterized by its typical layered rock-salt structure, which suggests anisotropic ionic conduction. LCO thin films with controlled orientations are valuable model for studying structural modification upon cycling and electrochemical performances, mainly in term of Li^+ diffusion. Kawashima et al. (2020) deposited epitaxial LCO thin film

TABLE 1 Experimental conditions for PLD of cathodes, anodes and electrolytes.

Cathode	Lasers source ((pulse regime), λ, repetition rate, fluence/ power)	Deposition conditions	References
MoO_3 (MO)	KrF (ns), 248 nm, 5 Hz, 1.5 J/cm^2	Target: MO 400°C, target-substrate distance (d) = 50 mm, p(O_2) from 2 to 20 Pa	Wei et al. (2023)
MoO3	Nd:YAG (ns), 266 nm, 2.5 J/cm^2	Target: Mo 450°C, d= 10 mm, p(O_2) = 0.5 mbar, 120 min	Trzciński et al. (2023)
V_2O_3 and Sn-doped V2O3	KrF (ns), 248 nm, 10 Hz, 1 J/cm^2	Target: V_2O_5 and V_2O_5+ 5wt% SnO_2, d=50 mm, p (N_2/O_2, 1:1) = 10^{-1} mbar	Tite et al. (2023)
V_2O_5 and V_2O_5-Au nanocomposite	KrF (ns), 248 nm, 10 Hz, 10 J/cm2	Target: V_2O_5 and V_2O_5-Au, RT, d=4.5 cm, p(O_2)= 13.3 Pa, 30 min	Hongliang et al. (2021)
$LiMn_2O_4$ (LMO)	KrF (ns), 248 nm, 10 Hz	Target: $LiMn_2O_4$ + Li_2O 650°C, d= 90 mm, p(O_2) = 20 mTorr	Erinmwingbovo et al. (2020)
$LiMn_2O_4$	KrF (ns), 248 nm, 1.3 J/cm^2	Target: $LiMn_2O_4$ and Li_2O, 650°C, d= 90 mm, p(O_2) =20 mTorr	Siller et al. (2022)
$Li_xMn_2O_4$	Nd:YAG (ns), 266 nm, 10 Hz, 0.6 W	Target: LiMn2O4 390°C or 500°C, p(O_2) =20 Pa	Kuwata et al. (2022)
$LiMn_2O_4$	KrF (ns), 248 nm, 5 Hz, 140 mJ/pulse	Target: $LiMn_2O_4$ 400°C, p(O_2) = 75 mTorr	Torres-Castanedo et al. (2024)
Li_2MnO_3	KrF (ns), 248 nm, 3 or 5 Hz, 1.1 J/cm^2	Target: $Li_{2.1}MnO_3$ and $Li_{2.4}MnO_3$ 973 K, d= 60 mm, p(O_2) = 50 or 75 Pa, 10 or 20 min	Hikima et al. (2021)
$LiCoO_2$ (LCO)	KrF (ns), 248 nm, 2.1 J/cm^2	Target: LCO + Li_2O (10:1) 500°C, d=35 mm, p(O_2)= 0.2 mbar	Pan et al. (2020)
$LiCoO_2$	Nd:YAG (ns), 266 nm, 100 kHz, 10^{15} W/m^2	Target: LCO, from RT to 550°C, d= 57 mm, 0.1 Pa or 5x10^{-4} Pa	Yuan et al. (2022)
$LiCoO_2$	KrF (ns), 248 nm, 5 or 20 Hz	Target: LCO from RT to 700°C, p(O_2)= 10^{-4} Pa–10 Pa	Kawashima et al. (2020)
$LiNi_{1/3}Mn_{1/3}Co_{1/3}O_2$ (NMC)	KrF (ns), 248 nm, 5 Hz, 0.7 J/cm^2, 20 ns	Target: $Li_{1.2}Ni_{1/3}Mn_{1/3}Co_{1/3}O_{2+\delta}$ 600°C, d=47 mm, p(O_2) = 100 mTorr	Nishio et al. (2020)
$LiNi_{1/3}Mn_{1/3}Co_{1/3}O_2$	Nd:YAG (ns), 266 nm, 10 Hz, 20 mJ	Target: $LiNi_{1/3}Mn_{1/3}Co_{1/3}O_2$ with 50% excess Li 923–1043 K, d= 40 mm, p(O_2) = 0.1–20 Pa, 50 min	Ohashi et al. (2021)
$LiMn_{0.5}Ni_{0.3}Co_{0.2}O_2$ (NMC 532)	KrF (ns), 248 nm, 5 Hz, 1.9 J/cm^2	Target: NMC532 + 15% Li_2CO_3 550°C, d= 5 cm, p(O_2) = 10 mTorr, 33 min	Qi et al., 2021
$LiMn_{1.5}Ni_{0.5}O_4$ (LMNO)	KrF (ns), 248 nm, 1 Hz, 1.7 J/cm^2	Target: LMNO 600°C, d= 7.5 cm, p(O_2) = 3.8x10^{-6} mbar or 4.6x10^{-3} mbar	Subash et al. (2024)
$LiCoO_{0.5}Ni_{0.}45Ag0.05O_2$ (LCNAO)	Nd:YAG (ns), 532 nm, 1 Hz, 1.94 J/cm^2, 10 ns	Target: LCNAO	Haider et al. (2020)
$LiCr_{1/6}Mn_{1/6}Fe_{1/6}Co_{1/6}Ni_{1/6}Cu_{1/6}O_2$ (HEO)	KrF (ns), 248 nm, 5 Hz, 0.93–1.35 J/cm^2	Target: HEO with excess Li 500°C–800°C, d= 47 mm, *p*= 1.3x10^{-1} Pa	Wang et al. (2022)
$LiFePO_4$	KrF (ns), 248 nm, 10 Hz, 10J/m^2	Target: LiFePO4 d= 4 cm, p(O2)	Koutavarapu et al. (2020)
Ternary metal fluoride Cu-Fe-F (CFF)	KrF (ns), 248 nm, 5 Hz, 2.5 J/cm^2	Target: CuF_2+FeF_3 (1:1) 400°C, d= 50 mm, p= 5x10^{-4} Pa, 30 min	Li et al. (2020)
Composite LiF-MxOy 4LiF/$NiFe_2O_4$ 4LiF/ $NiFe_2O_3$ 4LiF/NiO	KrF (ns), 248 nm, 2.5 J/cm^2	Target: LiF + $NiFe_2O_4$, LiF+ $NiFe_2O_3$, LiF + NiO 400°C, d= 50 mm, p(Ar) = 2 Pa, 30 min	Wei et al. (2021)
$NaFe_{0.5}Mn_{0.5}O_2$	KrF (ns), 248 nm, 10 Hz, 1.71 J/cm^2	Target: $NaFe_{0.5}Mn_{0.5}O_2$ 600°C, d= 35 mm, p(O_2) = 1.33x10^{-1} mbar	Nayak et al. (2020)
Na-Fe-Mn-O (NFMO)	KrF (ns), 248 nm, 10 Hz, 1.71 J/cm^2	Target: NFMO 400,500,600°C, d= 3.5 cm, p(O_2) = 1.33x10^{-1} mbar	Nayak et al. (2021)

(Continued on following page)

TABLE 1 (*Continued*) Experimental conditions for PLD of cathodes, anodes and electrolytes.

Cathode	Lasers source ((pulse regime), λ, repetition rate, fluence/ power)	Deposition conditions	References
$Na_{2/3}Ni_{1/4}Mn_{3/4}O_2$ (NNMO)	KrF (ns), 248 nm, 50 Hz, 1.5–31 J/cm^2	Target: NNMO, substrate: SS 750°C, d= 50 mm, p(O2) = 35,50,65 Pa	Lin et al. (2022)
Anodes	**Lasers source ((pulse regime), λ, repetition rate, fluence/ power)**	**Deposition conditions**	**References**
SnO_2	KrF (ns), 248 nm, 10Hz, 350 mJ	300°C–500°C, d = 4cm, p(O_2) =300 mTorr	Biswal et al. (2021)
SnO_2/TiO_2	KrF (ns), 248 nm, 300mJ, 5 Hz	RT	Wang et al. (2020)
$LiFe_5O8$	KrF (ns), 248 nm, 400 mJ	700°C, p(O_2) =4.6x10^{-3} mbar	Subash et al. (2023)
TiO_2/C	Nd:glass (fs), 527 nm, 2.8 mJ, 10 Hz	RT and post annealing at 200°C–800°C, 10^{-4} Pa, d=3 cm	Curcio et al. (2021)
BN	KrF (ns), 248 nm, 5 Hz, 2J/cm^2	RT, p(Ar) 50 mTorr, d =8 cm	Li et al. (2021)
Al_2O_3	Nd:YAG (ns), 266 nm, 10 Hz, 22 mJ	RT, 0.33Pa, d =4.5 cm	Kakimi et al. (2023)
Electrolyte	**Lasers source ((pulse regime), λ, repetition rate, fluence/ power)**	**Deposition conditions**	**References**
Ta-doped $Li_7La_3Zr_2O_{12}$ (Ta-LLZO)	KrF (ns), 248 nm, 10 Hz, 1.67 J/cm^2	Target: Ta-LLZO and Li_3N 300°C, d= 70 mm, p(O_2)= 1.3 Pa (Ta-LLZO) and 4 Pa (Li_3N)	Morozov et al. (2022)
$Li_{6.75}La_3Zr_{1.75}Ta_{0.25}O_{12}$ (LLZTO)	Nd:YAG (ns), 532 nm, 10 Hz, 10 ns, 30 J/cm^2	Target: LLZTO, LLZTO +6 wt% Li_2O RT, *p*= 10^{-3} Pa or p(O_2)= 10 Pa, d= 2cm, 3 h	Curcio et al. (2023)
Li_3PO_4	ArF (ns), 193 nm, 5 Hz, 1 J/cm^2	Target: Li_3PO_4	Nishio et al. (2020)
Li_3PO_4	ArF (ns), 193 nm, 5 Hz, 1 J/cm^2	Target: Li3PO4 RT, p= 4x10^{-6} Pa	Wang et al. (2022)
Li_3PO_4	ArF (ns), 193 nm, 150 mJ	RT, p(O_2) = 0.2 Pa	Kuwata et al. (2022)
$Li_{1+x}Al_xTi_{2-x}(PO_4)_3$ (LATP)	KrF (ns), 248 nm, 50 Hz, 1.4 J/cm^2	Target: LATP 700°C, d= 90 mm, p(O^2) = 80 mTorr	Siller et al. (2021)
LL(Nb,Ti)O-(Ti,Nb)O_2	KrF (ns), 248 nm, 8 Hz, 1.0 J/cm^2	Target: $Li_{3x}La_{2/3-x}(Nb_{0.7}Ti_{0.32})O_3$ 880°C, d= 45 mm, p(O_2)= 10 Pa	Lovett et al. (2022)
La_2LiHO_3 (LLHO)	Nd:YAG (ns), 266 nm, 3.33 Hz, 0.1–0.2 J/cm^2	Target: LLHO +180% LiH 400°C–700°C, d= 40 mm, p(H_2) = 1.3 Pa	Sasahara et al. (2023)

cathodes with two different orientation, revealing a significant disparity in Li-ion diffusion rates between (104)-oriented and c-axis oriented LCO cathodes. This discrepancy arises from the orientation of the diffusion channels: while c-axis oriented films impede diffusion due to parallel alignment with the solid electrolyte and obstruction by CoO_2 planes, (104)-oriented films facilitate charge transport by direct exposure to the electrolyte (Kawashima et al., 2020). Pan et al. (2020), instead, deposited (003)-oriented LCO, demonstrating the presence of diffusion-controlled reversible capacity loss in layered oxide cathodes, which can be recovered with extended Li diffusion time during the lithiation process. On the other hand, Yuan et al. (2022) proposed a novel high-speed PLD process for large-scale fabrication of crystalline (001)-oriented LCO by using a high repetition rate 1,064 nm Nd:YAG fiber laser. They deposited at various deposition temperature (RT, 300, 350, 400, 450, 500, and 550°C) in order to investigate the effect of the deposition temperature on the film crystallinity and, as a consequence, on the electrochemical performances. The crystallinity of the films was too low up to 400 °C, therefore, electrochemical tests were conducted in cell vs. Li^+/Li for films deposited at 450, 500, and 550 °C, demonstrating that the film with the highest crystallinity, deposited at 550 °C, exhibited the highest specific capacity. Additionally, the researchers investigated the effect of film thickness by depositing films at 550°C for varying deposition time to achieve thicknesses of 0.27, 0.65, and 1.31 microns. It was confirmed that thinner films showed superior electrochemical performance, attributed to enhanced lithium ion mobility in a reduced diffusion pathway typical of 2D films. Similarly to LCO, lithium nickel manganese cobalt oxides (NMC) possesses a layered rock-salt crystal structure and is one of the most widely used cathode materials for high-power batteries to date. However, its application in solid-state batteries still requires studies to analyze the cathode-electrolyte interface resistance. In this regard, Nishio et al. (2020) deposited (104)- and (001)-oriented NMC epitaxial thin films and analyzed interface resistance with Li_3PO_4 thin film electrolyte (similarly deposited via laser), founding low interface resistance values for both the cathodes (5.2 and 10.2 Ω/cm^2, respectively). Whereas, Ohashi et al. (2021) tuned deposition parameters to obtain (003)-oriented NMC, used for a simultaneous

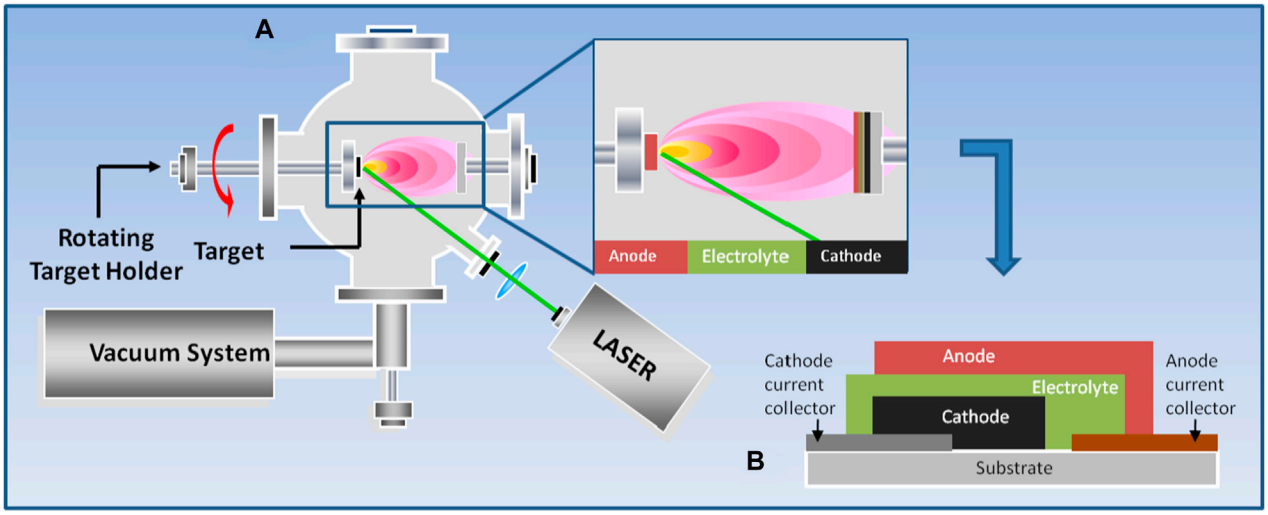

FIGURE 1
Schematic illustration of: **(A)** PLD experimental set-up **(B)** thin film microbattery cross-section.

electrochemical analysis with regular NMC electrode, demonstrating how the thin film one can be utilized as a model for studying charge transfer processes at the electrode-electrolyte interface.

Similarly to NMC, other layered rock-salt cathode materials containing different transition metals have also been deposited via PLD (Haider et al., 2020; Wang et al., 2022; Subash et al., 2024). Among these, thin films of $LiMn_{1.5}Ni_{0.5}O_4$ (LMNO) exhibited high Li diffusion coefficients (10^{-5}–10^{-6} cm^2/s) and excellent cyclability in a wide current range (Subash et al., 2024). While Wang et al. (2022) deposited a high-entropy oxide (HEO) with a higher number of transition metals: $LiCr_{1/6}Mn_{1/6}Fe_{1/6}Co_{1/6}Ni_{1/6}Cu_{1/6}O_2$. They deposited an epitaxial thin film by tuning deposition temperature and laser fluence. Such film was used in a HEO/Li_3PO_4/Li thin film cell, however a large interface resistance was measured, therefore a anisotropic structure has to be evaluated for this material.

2.1.2 Phosphates

While for the PLD of intercalation cathode materials based on transition metal oxides, as seen so far, there are several studies in the recent literature, only one paper concerns the PLD of phosphates and a couple is on fluorides (conversion cathodes). In particular, Koutavarapu et al. (2020) deposited $LiFePO_4$ (LFP) in oxygen atmosphere, obtaining a film of LFP with minor amount of lithium and iron oxides, even though high specific capacity and capacity retention were obtained vs. Li^+/Li.

2.1.3 Metal fluorides

Conversion cathodes based on metal fluoride are attractive for their high capacity and voltage, however their structural reorganization during conversion reaction causes high volumetric changes and thus scarce capacity retention and reversibility. Therefore, two different composite conversion cathodes, in which volume changes were limited, were developed and deposited in form of thin film as a model to study their conversion reaction. A ternary metal fluoride Cu-Fe-F (CFF) cathode, obtained by co-deposition of $CuFe_2$ an FeF_3 targets, demonstrated a reversible structural rearrangement upon cycling leading to high reversibility and columbic efficiency (Li et al., 2020). Alternatively, Wei et al. (2021) deposited different LiF/Fe_2O_3, LiF/NiO, and LiF/$NiFe_2O_4$ films by PLD of a composite targets with different LiF/MO_x ratio. Among these, 4LiF/$NiFe_2O_4$ shown the best electrochemical performances in term of cycling stability and rate capability thanks to the reversible splitting and regeneration of LiF, as well as the adsorption and desorption of F^- at the redox center of $NiFe_2O_4$.

2.2 Cathodes for sodium ion batteries

While lithium-based thin-film batteries have been extensively studied, research on sodium-based microbatteries remains limited. Thin-film batteries exhibit superior ion diffusion kinetics, resulting in enhanced cyclic performance and increased energy density compared to conventional rechargeable batteries. This is particularly important for SIBs, as sodium has larger dimensions than lithium, making intercalation/deintercalation processes more challenging. Nayak et al. (Nayak et al., 2020; Nayak et al., 2021) deposited a Na-Fe-Mn-O (NFMO) thin films at 400, 500, and 600°C, evidencing how film quality is dependent on deposition temperature. The best film, obtained at 600°C, shown high capacity and Coulombic efficiency (>91% after 1,500 cycles). On the contrary, Lin J. et al. (2020) analyzed the effect of the pressure of oxygen ($p(O_2)$): 35, 50, 65 Pa) during the deposition of $Na_{2/3}Ni_{1/4}Mn_{3/4}O_2$ (NNMO). Film deposited at higher pressure exhibited higher sodium storage, better capacity and cycling performance (Lin et al., 2022).

3 Anodes

With respect to negative electrodes for secondary batteries, few studies were published in the last years. Commercial anodes for LIBs involve the use of graphite, but its theoretical capacity is too low for the development of high energy density batteries suitable for

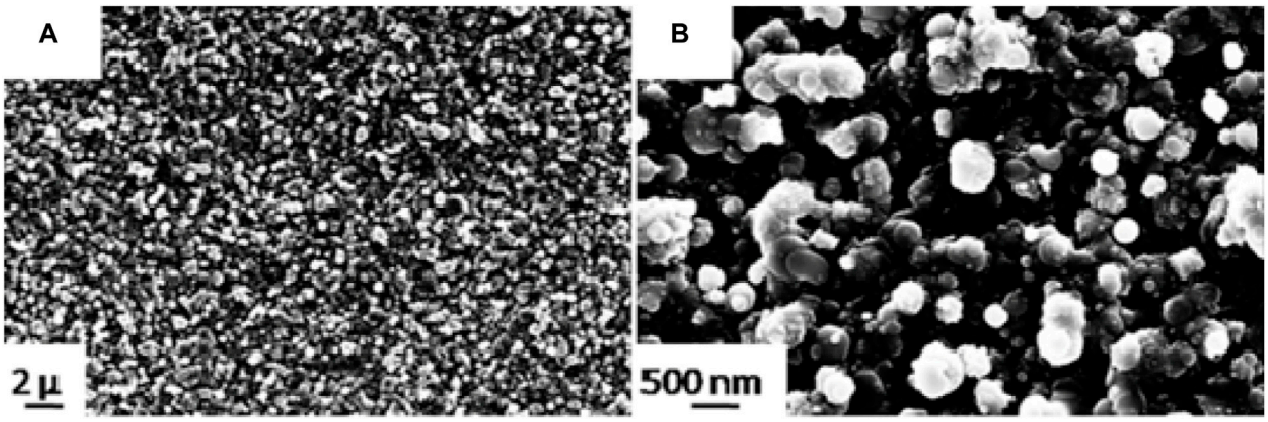

FIGURE 2
SEM images at two different magnification **(A,B)** of TiO2 films deposited by femtosecond laser ablation (Reproduced with permission from Curcio et al. (2021), copyright from 2021 Elsevier).

microelectronic or medical devices. Metallic lithium has high theoretical energy density (−3,680 mAh/g) and low reduction potential (−3.04 V vs. standard hydrogen potential) and can serve as anode for Li Metal Batteries (LMB). However, it presents some serious safety concerns due to the dendrite propagation during the battery cycle life. To tackle the anode issue, thin, dense films of transition metal oxides or multielemental oxides were grown by PLD to serve as anodes or to protect highly reactive anodes. Lithium ferrite nanostructures have been considered as low cost and environmental friendly material. Subash et al. (2023) grown crystalline $LiFe_5O_8$ films with a thickness of about 100 nm. The ordered ferrite thin films present a specific discharge capacity of 25 µAh/cm^2 and current density of 10 µA/cm^2, suggesting their potential use for fabricating sustainable solid batteries.

The capability of PLD technique to deposit films with controlled thickness and morphology resulted useful to study and to limit processes that negatively affect the performances of electrochemical cells such as lithium dendrite growth. In fact, to mitigate the formation and propagation of dendrite that are detrimental for the battery stability Li et al. (2021) deposited on the anode surface a electrically insulating and ionically conductive BN film of about 1.2 µm. The BN film, deposited in argon atmosphere at a pressure of 50 mTorr posses a 3D hierarchical structure providing free space for Li accommodation during Li stripping and plating. The mechanisms involved in the beneficial effect of the coating of Li anodes with Al_2O_3 films were deeply investigated by Kakimi et al. (2023). By depositing smooth Al_2O_3 layers with controlled thickness, the authors compare the cycling stability of coin cells with coated and uncoated electrodes. The Al_2O_3 film thickness was adjusted varying the deposition time from 1 to 3 h, obtaining films 15 nm and 82 nm thick, respectively. The authors observed that the thinner Al_2O_3 coatings assure a more efficient reaction of lithium deposition-dissolution. In fact, lithium grows with a plate-like morphology on the coated electrode, ensuring a good electronic conduction between the electrode and the deposited lithium that is mainly removed from the electrode surface during the dissolution cycle. Moreover, XPS analysis of the coated and uncoated electrodes after cycling, highlight the Al_2O_3 films are able to suppress the formation of lithium carbonate arising for the electrolyte decomposition.

Since TiO_2 have a negligible volume variation during Li intercalation-deintercalation, anatase anodes have been proposed for long cycle life batteries. Although TiO_2 is a low cost and non toxic materials, its major drawbacks are the poor electronic and ionic conductivities. Various strategies have been proposed to overcome these disadvantages, such as combining with other oxides like SnO_2, which has a higher specific capacity. The deposition of a multilayered SnO_2/TiO_2 has been proposed by Wang et al. (2020). The layered anode was grown alternating SnO_2 and TiO_2 layers (20 nm and 5 nm thick, respectively) for total thickness of 300 nm. Since the deposition experiments were carried out at room temperature, authors suggest that the electrode's amorphous structure can play a beneficial role in its electrochemical performances, in particular considering the cycle stability. In fact, the surface of the coated electrode is characterized by a morphology without any cracks after 200 cycles. A different strategy proposed to overcome the drawbacks of TiO_2 that limit its industrial applications is to tailor size and morphology of TiO_2-based materials. With respect to the possibility to reduce the TiO_2 morphology at the nanoscale, it is well known that during the ablation with femtosecond laser source the ejection of nanoparticles that retains the target stoichiometry take place, getting to the growth of films with a nanomorphology very different with respect to films obtained by nanosecond ablation (De Bonis and Teghil, 2020). To obtain compact, dense and nanostructured TiO_2 films (Figure 2), femtosecond laser ablation of an anatase target has been proposed (Curcio et al., 2021). The authors studied the deposition mechanism and developed and characterised a TiO_2/C layered anode suitable for microbatteries with lower charge transfer resistance, higher apparent Li^+ diffusion and better cycling stability than reference microelectrodes.

SnO_2 is an efficient anode for SIBs, but the high volume change during cycling due to Na insertion and de-insertion leads to cracking and degradation of electrochemical performance. Biswal et al. (2021) demonstrated the role of the morphology and crystallinity of SnO_2 films on the cycling properties of SIBs. They deposited films at

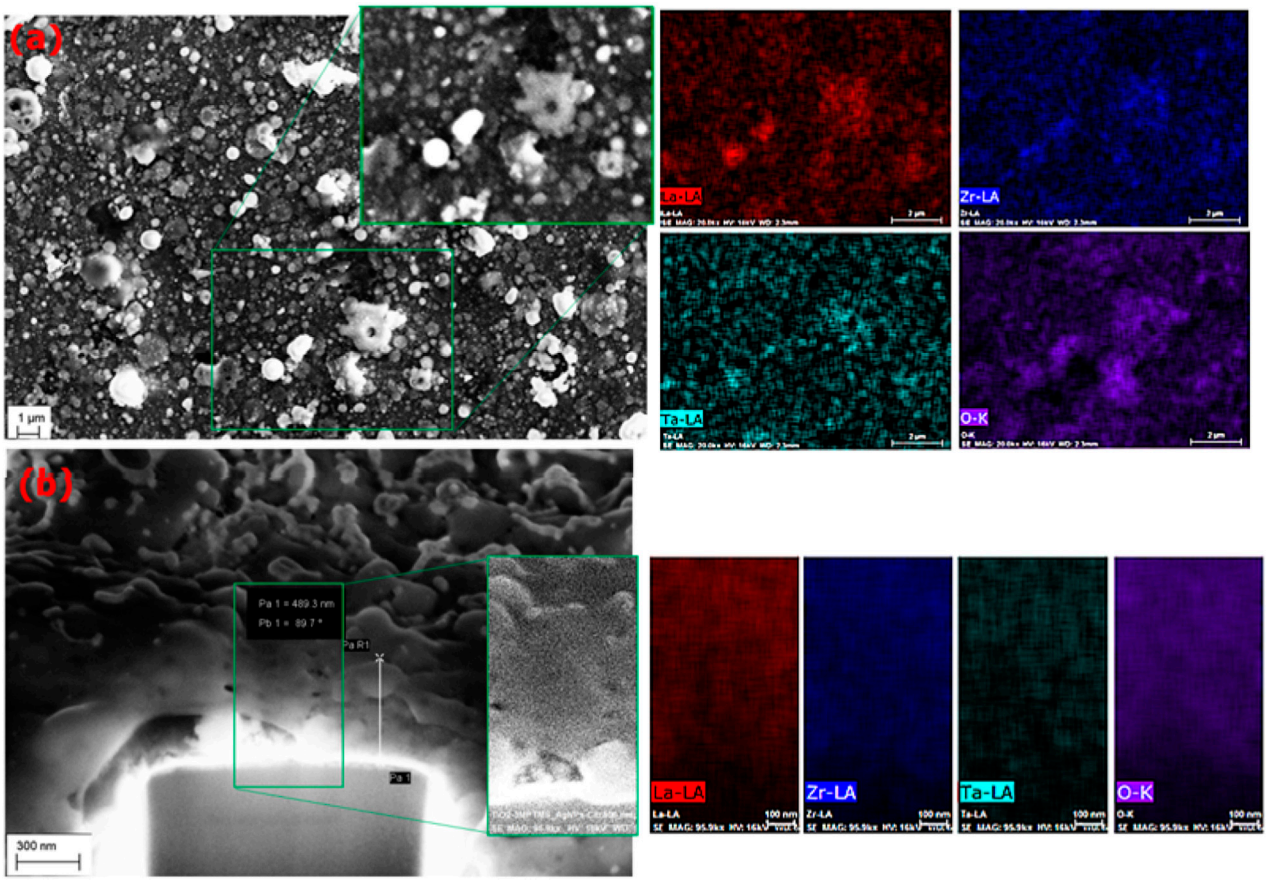

FIGURE 3
LLZTO film deposited by nanosecond PLD at a pressure of 10 Pa of O_2 and room temperature **(A)** and its cross-section **(B)** with elemental mapping (Reproduced from Curcio et al. (2023)).

different substrate temperature (300, 400°C and 500°C) with a "cauliflower-like" morphology. With increasing the temperature the nanograins of the structure tend to aggregate and their crystallite size tends to increase as shown by SEM and XRD analysis, respectively. The authors show that the presence of an amorphous phase and nanograin morphology has a positive effect on the film's ability to resist volume changes, improving its stability compared to crystalline films.

4 Electrolytes

The use of all-state batteries is a promising alternative to conventional batteries. In particular, the use of solid electrolytes (SEs) offers a number of advantages, including higher energy and power density, as well as improved safety. SEs are mainly divided into polymer-based and inorganic types, which include garnets, LISICON, NASICON, and perovskites. As regards garnet $Li_7La_3Zr_2O_{12}$ (LLZO) a couple of study are focused on the deposition of Ta-doped LLZO, since doping with La stabilizes the cubic form of LLZO, which exhibits higher Li conductivity. In both of them, Ta-doped LLZO target material was enriched in Li content to balance the inevitable Li loss during deposition. Curcio et al. (2023) deposited 2D films at different deposition pressure and post deposition heat treatment. Crystalline LLZTO film was deposited at 10 Pa of O_2 at RT (Figure 3), while post deposition treatment caused Li-poor phase formation (Curcio et al., 2023). While Morozov et al. (2022) studied the correlation among deposition conditions and the microstructure at the interface between LCO and Ta-doped LLZO deposited via PLD.

There are several studies regarding the PLD of lithium phosphates electrolytes (Nishio et al., 2020; Kuwata et al., 2022; Wang et al., 2022), but all investigate only the cathode component in contact with such SE in the form of thin film. Only in one case the properties of a NASICON film are studied. They obtained dense thin films of $Li_{1+x}Al_xTi_{2-x}(PO_4)_3$ (LATP) at high temperature (700°C) and deposition pressure (80 mTorr), however only after post deposition treatment at 800°C the ionic conductivity increased up to 10^{-4} S/cm, thanks to the improved contact between crystallites with different orientation as a consequence of the formation of amorphous phase at the grain boundaries (Siller et al., 2021).

Lovett et al. (2022) deposited a vertically aligned nanocomposite of two perovskite-based electrolyte, i.e., $Li_{3x}La_{2/3-x}TiO_3$ (LLTO) and $Li_{3x}La_{2/3-x}NO_3$ (LLNO), together with an anodic material: LL(Nb,Ti)O-(Ti,Nb)O_2-anatase. LL(Nb,Ti)O-(Ti,Nb)O_2 film grew epitaxially with high purity and crystallinity on an Nb-STO substrate, exhibiting ion conductivity ($2.3x10^{-4}$ S/cm) an order of

magnitude higher than bulk LLNO and comparable to the best LLTO film obtained.

Lastly new SE based on hydrides was proposed, in which the lightweight hydrogen atoms in polyanions facilitates their rotation, enabling effective ion transfer through the paddle-wheel mechanism (Pang et al., 2022). Additionally, the highly reductive nature of $H^{\delta-}$ enhances compatibility with metal anodes and leads to more suitable interphases. In particular, Sasahara et al. (2023) deposited a single phase (001)-oriented La_2LiHO_3 epitaxial thin film with an ionic conductivity of $1.3x10^{-8}$ S/cm, an order of magnitude higher than bulk form.

5 Conclusion and outlooks

We have reviewed the most recent study on the preparation of thin films for cathodes, electrolytes and anodes for microbatteries application by PLD technique. In order to optimize the electrochemical performances of the deposited electroactive films, the deposition time has been varied, whereas films morphology strongly depends on the properties of the laser source, mainly the laser pulse length. The films' crystallite size can be controlled varying the temperature of the substrate during the deposition experiments, but it has been show that anodes formed by amorphous films has higher stability with respect to crystalline one due to their capability to resist to volume changes during the intercalation-deintercalation process (Biswal et al., 2021). The ability to finely control the thickness and orientation of crystals in coatings makes it possible to grow model electrodes that have been used to study electrochemical reactions in cells.

PLD is recognized has the technique of choice for deposition of coatings with complex composition, on the other hand the lithium loss during the growth of cathodes and electrolytes thin films require a deep knowledge and a careful control of the deposition conditions and can lead to materials with diminished performances.

Finally, the capability to perform electrochemical characterization of films containing lithium *in situ*, avoiding air/moisture exposure, holds significant importance and would represent a substantial advancement in the research, facilitating the comparison of data obtained from different laboratories.

Author contributions

MC: Writing–original draft, Writing–review and editing. RT: Writing–original draft, Writing–review and editing. AD: Writing–original draft, Writing–review and editing.

Funding

The author(s) declare that financial support was received for the research, authorship, and/or publication of this article. This work was funded by the Next-Generation EU–Italian NRRP, Mission 4, Component 2, Investment 1.5, call for the creation and strengthening of "Innovation Ecosystems", building "Territorial R&D Leaders" (Directorial Decree n. 2021/3277)–project Tech4You–Technologies for climate change adaptation and quality of life improvement, n. ECS0000009. This work reflects only the authors' views and opinions, neither the Ministry for University and for Research nor the European Commission can be considered responsible for them.

Conflict of interest

The authors declare that the research was conducted in the absence of any commercial or financial relationships that could be construed as a potential conflict of interest.

The author(s) declared that they were an editorial board member of Frontiers, at the time of submission. This had no impact on the peer review process and the final decision.

Publisher's note

References

Biswal, R., Nayak, D., Janakiraman, S., Chaudhary, N. V. P., Ghosh, S., and Adyam, V. (2021). Revisiting and enhancing electrochemical properties of SnO2 as anode for sodium-ion batteries. *J. Solid State Electrochem.* 25, 561–573. doi:10.1007/s10008-020-04779-9

Curcio, M., Brutti, S., Celeste, A., Galasso, A., De Bonis, A., and Teghil, R. (2023). Influence of deposition conditions and thermal treatments on morphological and chemical characteristics of $Li_{6.75}La_3Zr_{1.75}Ta_{0.25}O_{12}$ thin films deposited by nanosecond PLD. *Coatings* 13, 1496. doi:10.3390/coatings13091496

Curcio, M., De Bonis, A., Brutti, S., Santagata, A., and Teghil, R. (2021). Pulsed laser deposition of thin films of TiO2 for Li-ion batteries. *Appl. Surf. Sci. Adv.* 4, 100090. doi:10.1016/j.apsadv.2021.100090

De Bonis, A., and Teghil, R. (2020). Ultra-short pulsed laser deposition of oxides, borides and carbides of transition elements. *Coatings* 10 (5), 501. doi:10.3390/coatings10050501

Erinmwingbovo, C., Siller, V., Nuñez, M., Trócoli, R., Brogioli, D., Morata, A., et al. (2020). Dynamic impedance spectroscopy of LiMn2O4 thin films made by multi-layer pulsed laser deposition. *Electrochimica Acta* 331, 135385. doi:10.1016/j.electacta.2019.135385

Fenech, M., and Sharma, N. (2020). Pulsed laser deposition-based thin film microbatteries. *Chem. – Asian J.* 15, 1829–1847. doi:10.1002/asia.202000384

Haider, A. J., Rsool, R. A., Haider, M. J., Rsool, R. A., and Dheyab, A. B. (2020). Properties of $LiCo_{0.5}Ni_{0.45}Ag_{0.05}O_2$ thin films for high storage energy capacity by Pulsed Laser Deposition. *Energy Rep.* 6, 85–94. doi:10.1016/j.egyr.2020.08.028

Hikima, K., Taminato, S., Hinuma, Y., Shimizu, K., Suzuki, K., Hirayama, M., et al. (2021). Influence of chemical composition and domain morphology of Li_2MnO_3 on battery properties. *Batter. Supercaps* 4 (3), 493–503. doi:10.1002/batt.202000251

Hongliang, L., Kaiyuan, W., Zi, Y., Quanchao, Z., and Yanhua, C. (2021). V_2O_5-Au nanocomposite film cathode with enhanced electrochemical performance for lithium-ion micro batteries. *Chem. Phys.* 544, 111111. doi:10.1016/j.chemphys.2021.111111

Indrizzi, L., Ohannessian, N., Pergolesi, D., Lippert, T., and Gilardi, E. (2021). Pulsed laser deposition as a tool for the development of all solid-state microbatteries. *Helvetica Chim. Acta* 104 (2), e2000203. doi:10.1002/hlca.202000203

Julien, C. M., and Mauger, A. (2019). Pulsed laser deposited films for microbatteries. *Coatings* 9 (6), 386. doi:10.3390/coatings9060386

Kakimi, T., Miyakawa, S., Taminato, S., Saito, T., Mori, D., and Imanishi, N. (2023). Mechanistic study of Al2O3 coating effects on lithium deposition and dissolution reaction. *RSC Adv.* 13, 9142–9153. doi:10.1039/D2RA08027C

Karimzadeh, S., Safaei, B., Yuan, C., and Jen, T. (2023). Emerging atomic layer deposition for the development of high-performance lithium-ion batteries. *Electrochem. Energy Rev.* 6, 24. doi:10.1007/s41918-023-00192-8

Kawashima, K., Ohnishi, T., and Takada, K. (2020). High-rate capability of $LiCoO_2$ cathodes. *ACS Appl. Energy Mater.* 3 (12), 11803–11810. doi:10.1021/acsaem.0c01973

Koutavarapu, R., Shim, J., and Rao, M. C. (2020). Substrate effect on structural and electrochemical properties of LiFePO4 thin films grown by pulsed laser deposition. *J. Mat. Sci. Mat. Electron.* 31, 5040–5046. doi:10.1007/s10854-020-03037-y

Kuwata, N., Matsuda, Y., Okawa, T., Hasegawa, G., Kamishima, O., and Kawamura, J. (2022). Ion dynamics of the Li Mn2O4 cathode in thin-film solid-state batteries revealed by *in situ* Raman spectroscopy. *Solid State Ionics* 380, 115925. doi:10.1016/j.ssi.2022.115925

Li, G., Li, H., Wang, Y., Xiong, D., Wang, S., Yan, Y., et al. (2021). Suppressing Li dendrite puncture with a hierarchical h-BN protective layer. *Acs. Appl. Mat. Interfaces* 13 (47), 56109–56115. doi:10.1021/acsami.1c15980

Li, J., Xu, L., Wei, K., Ma, S., Liu, X., Zhao, Y., et al. (2020). *In situ* forming of ternary metal fluoride thin films with excellent Li storage performance by pulsed laser deposition. *Ionics* 26 (7), 3367–3375. doi:10.1007/s11581-020-03528-2

Lin, B., Dai, W., Tao, J., Li, J., Wang, C., Zhao, Y., et al. (2022). Excimer laser-deposited Na2/3Ni1/4Mn3/4O2 film cathode for stable sodium-ion battery. *Nanomaterials* 12 (17), 3018. doi:10.3390/nano12173018

Lovett, A. J., Kursumovic, A., Dutton, S., Qi, Z., He, Z., Wang, H., et al. (2022). Lithium-based vertically aligned nanocomposite films incorporating $Li_xLa_{0.32}(Nb_{0.7}Ti_{0.32})O_3$electrolyte with high Li^+ ion conductivity. *Apl. Mater.* 10 (5), 0–7. doi:10.1063/5.0086844

Morozov, A. V., Paik, H., Boev, A. O., Aksyonov, D. A., Lipovskikh, S. A., Stevenson, K. J., et al. (2022). Thermodynamics as a driving factor of LiCoO2Grain growth on nanocrystalline Ta-LLZO thin films for all-solid-state batteries. *ACS Appl. Mat. Interfaces.* 14 (35), 39907–39916. doi:10.1021/acsami.2c07176

Nayak, D., Ghosh, S., and Venimadhav, A. (2021). Structural and electrochemical kinetics of Na–Fe–Mn–O thin-film cathode: a synergistic effect of deposition conditions. *Ionics* 27 (6), 2421–2430. doi:10.1007/s11581-021-04043-8

Nayak, D., Majumder, S., Ghosh, S., and Adyam, V. (2020). Superior electrochemical performance of $NaFe_{0.5}Mn_{0.5}O_2$ thin film electrode fabricated by pulse laser deposition. *Mater. Today Proc.* 33, 5425–5428. doi:10.1016/j.matpr.2020.03.138

Nishio, K., Nakamura, N., Horiba, K., Kitamura, M., Kumigashira, H., Shimizu, R., et al. (2020). Impact of the crystal orientation of positive electrodes on the interface resistance across a solid electrolyte and electrode. *ACS Appl. Energy Mater.* 3 (7), 6416–6421. doi:10.1021/acsaem.0c00644

Ohashi, T., Hirano, T., Okazaki, K., Fukunaga, T., and Abe, T. (2021). Hysteresis of the charge transfer resistance between the charge and discharge processes obtained from electrochemical impedance measurements using a thin-film cathode for a lithium-ion cell. *J. Electroanal. Chem.* 899, 115675. doi:10.1016/j.jelechem.2021.115675

Pan, R., Rau, D., Moryson, Y., Sann, J., and Janek, J. (2020). Reversible capacity loss of $LiCoO_2$Thin film electrodes. *ACS Appl. Energy Mater.* 3 (7), 6065–6071. doi:10.1021/acsaem.0c00819

Pang, Y., Liu, Y., Yang, J., Zheng, S., and Wang, C. (2022). Hydrides for solid-state batteries: a review. *Mater. Today Nano* 18, 100194. doi:10.1016/j.mtnano.2022.100194

Sasahara, Y., Hirose, T., Yoshimoto, M., Matsui, N., Kobayashi, S., Ubukata, H., et al. (2023). High H- conductivities along the ab-planes of La_2LiHO_3 epitaxial thin films. *Cryst. Growth and Des.* 23 (10), 7103–7108. doi:10.1021/acs.cgd.3c00376

Siller, V., Gonzalez-Rosillo, J. C., Eroles, M. N., Baiutti, F., Liedke, M. O., Butterling, M., et al. (2022). Nanoscaled $LiMn_2O_4$ for extended cycling stability in the 3 V plateau. *ACS Appl. Mat. Interfaces* 14 (29), 33438–33446. doi:10.1021/acsami.2c10798

Siller, V., Morata, A., Eroles, M. N., Arenal, R., Gonzalez-Rosillo, J. C., López Del Amo, J. M., et al. (2021). High performance LATP thin film electrolytes for all-solid-state microbattery applications. *J. Mat. Chem.A* 9 (33), 17760–17769. doi:10.1039/d1ta02991f

Subash, S., Lakshmanan, K., Vediappan, K., and Bharathi, K. K. (2024). High Li-ion diffusion coefficient in $LiMn_{1.5}Ni_{0.5}O_4$ thin films for all-solid Li-ion battery applications. *Appl. Phys. Lett.* 124 (2), 023903. doi:10.1063/5.0178190

Subash, S., Udhayakumar, S., Kumaresan, L., Patro, L. N., Kumaran, V., Kumar, E. S., et al. (2023). Ordered LiFe5O8 thin films prepared by pulsed laser deposition as an anode material for all-solid thin film batteries. *Electrochimica Acta* 454 (2023), 142318. doi:10.1016/j.electacta.2023.142318

Tite, T., Ungureanu, C., Buga, M., Stavarache, I., Matei, El., Catalin Negrila, C., et al. (2023). Pulsed laser deposited V_2O_3 thin-films on graphene/aluminum foil for micro-battery applications. *J. Electroanal. Chem.* 933, 117290. doi:10.1016/j.jelechem.2023.117290

Torres-Castanedo, C. G., Buchholz, D. B., Pham, T., Zheng, L., Cheng, M., Dravid, V. P., et al. (2024). Ultrasmooth epitaxial Pt thin films grown by pulsed laser deposition. *ACS Appl. Mat. Interfaces* 16, 1921–1929. doi:10.1021/acsami.3c16065

Trzciński, K., Zarach, Z., Szkoda, Ma., Nowak, A. P., Berent, K., and Sawczak, M. (2023). Controlling crystallites orientation and facet exposure for enhanced electrochemical properties of polycrystalline MoO_3 films. *Sci. Rep.* 13 (1), 16668. doi:10.1038/s41598-023-43800-9

Wang, K., Nishio, K., Horiba, K., Kitamura, M., Edamura, K., Imazeki, D., et al. (2022). Synthesis of high-entropy layered oxide epitaxial thin films: $LiCr_{1/6}Mn_{1/6}Fe_{1/6}Co_{1/6}Ni_{1/6}Cu_{1/6}O_2$. *Cryst. Growth and Des.* 22 (2), 1116–1122. doi:10.1021/acs.cgd.1c01076

Wang, W., Li, Y., Li, L., Wang, L., and Wang, K. (2020). SnO2/TiO2 nanocomposite prepared by pulsed laser deposition as anode material for flexible quasi-solid-state lithium-ion batteries. *Int. J. Electrochem. Sci.* 15, 11709–11722. doi:10.20964/2020.12.49

Wei, K., Qiu, J., Zhao, Y., Ma, S., Wei, Y., Li, H., et al. (2023). Tunable oxygen vacancies in MoO_3 lattice with improved electrochemical performance for Li-ion battery thin film cathode. *Ceram. Int.* 49 (13), 21729–21736. doi:10.1016/j.ceramint.2023.03.313

Wei, K., Zhao, Y., Chen, K., Sun, K., Wu, T., Dong, Z., et al. (2021). Low-overpotential LiF splitting in lithiated fluoride conversion cathode catalyzed by spinel oxide. *Adv. Funct. Mater.* 31 (18). doi:10.1002/adfm.202009133

Xia, Q., Zan, F., Zhang, Q., Liu, W., Li, Q., He, Y., et al. (2023). All-solid-state thin film lithium/lithium-ion microbatteries for powering the internet of things. *Adv. Mater.* 35, 2200538. doi:10.1002/adma.202200538

Yuan, K., Xie, M., Dong, W., Zhao, P., Pan, J., Liu, Z., et al. (2022). High-speed and one-step deposition of a LiCoO2thin-film electrode by a high-repetition 1064 nm Nd:YAG fiber laser. *ACS Appl. Energy Mater.* 5 (12), 15483–15490. doi:10.1021/acsaem.2c02826

Zhao, Y., Liu, Q., Zhao, X., Mu, D., Tan, G., Li, L., et al. (2023). Structure evolution of layered transition metal oxide cathode materials for Na-ion batteries: issues, mechanism and strategies. *Mater. Today* 62 (271), 271–295. doi:10.1016/j.mattod.2022.11.024